Affinity for phosphatidylinositol 4,5-bisphosphate determines muscarinic agonist sensitivity of Kv7 K^+ channels

Ciria C. Hernandez,[1] Björn Falkenburger,[2] and Mark S. Shapiro[1]

[1]Department of Physiology, University of Texas Health Science Center, San Antonio, TX 78229
[2]Department of Physiology and Biophysics, University of Washington School of Medicine, Seattle, WA 98195

Kv7 K^+-channel subunits differ in their apparent affinity for PIP_2 and are differentially expressed in nerve, muscle, and epithelia in accord with their physiological roles in those tissues. To investigate how PIP_2 affinity affects the response to physiological stimuli such as receptor stimulation, we exposed homomeric and heteromeric Kv7.2, 7.3, and 7.4 channels to a range of concentrations of the muscarinic receptor agonist oxotremorine-M (oxo-M) in a heterologous expression system. Activation of M_1 receptors by oxo-M leads to PIP_2 depletion through G_q and phospholipase C (PLC). Chinese hamster ovary cells were transiently transfected with Kv7 subunits and M_1 receptors and studied under perforated-patch voltage clamp. For Kv7.2/7.3 heteromers, the EC_{50} for current suppression was 0.44 ± 0.08 µM, and the maximal inhibition ($Inhib_{max}$) was 74 ± 3% (n = 5–7). When tonic PIP_2 abundance was increased by overexpression of PIP 5-kinase, the EC_{50} was shifted threefold to the right (1.2 ± 0.1 µM), but without a significant change in $Inhib_{max}$ (73 ± 4%, n = 5). To investigate the muscarinic sensitivity of Kv7.3 homomers, we used the A315T pore mutant ($Kv7.3^T$) that increases whole-cell currents by 30-fold without any change in apparent PIP_2 affinity. $Kv7.3^T$ currents had a slightly right-shifted EC_{50} as compared with Kv7.2/7.3 heteromers (1.0 ± 0.8 µM) and a strongly reduced $Inhib_{max}$ (39 ± 3%). In contrast, the dose–response curve of homomeric Kv7.4 channels was shifted considerably to the left (66 ± 8 nM), and $Inhib_{max}$ was slightly increased (81 ± 6%, n = 3–4). We then studied several Kv7.2 mutants with altered apparent affinities for PIP_2 by coexpressing them with $Kv7.3^T$ subunits to boost current amplitudes. For the lower affinity (Kv7.2 (R463Q)/$Kv7.3^T$) or higher affinity (Kv7.2 (R463E)/$Kv7.3^T$) channels, the EC_{50} and $Inhib_{max}$ were similar to Kv7.4 or $Kv7.3^T$ homomers (0.12 ± 0.08 µM and 79 ± 6% [n = 3–4] and 0.58 ± 0.07 µM and 27 ± 3% [n = 3–4], respectively). The very low-affinity Kv7.2 (R452E, R459E, and R461E) triple mutant was also coexpressed with $Kv7.3^T$. The resulting heteromer displayed a very low EC_{50} for inhibition (32 ± 8 nM) and a slightly increased $Inhib_{max}$ (83 ± 3%, n = 3–4). We then constructed a cellular model that incorporates PLC activation by oxo-M, PIP_2 hydrolysis, PIP_2 binding to Kv7-channel subunits, and K^+ current through Kv7 tetramers. We were able to fully reproduce our data and extract a consistent set of PIP_2 affinities.

The Journal of General Physiology

INTRODUCTION

A wide spectrum of ion channels and transporters are regulated by the plasma membrane abundance of the lipid phosphatidylinositol (PI) 4,5-bisphosphate (PIP_2). Upon stimulation of $G_{q/11}$-coupled receptors, activation of phospholipase Cβ hydrolyzes PIP_2, producing cytosolic inositol triphosphate (IP_3) and membrane-bound diacylglycerol, leading to three possible modes of action on ion channels: IP_3-mediated Ca^{2+}_i signals, diacylglycerol-mediated activation of protein kinase C, and depletion of PIP_2 via consumption by PLC activity (Gamper and Shapiro, 2007). M-type K^+ currents are produced by voltage-gated Kv7 (KCNQ) subunits in a variety of neuronal, muscle, and epithelial tissues, where they control excitability, action potentials, and K^+ transport (Jentsch, 2000; Delmas and Brown, 2005; Mackie and Byron, 2008; Peroz et al., 2008). In the nervous system, most M channels are composed of Kv7.2/7.3 heteromers, but some channels also contain Kv7.5, and Kv7.2 or Kv7.3 homomers are also neuronally expressed (Wang et al., 1998; Cooper et al., 2001; Roche et al., 2002; Pan et al., 2006). In the inner ear and auditory cortex, Kv7.4 homomers dominate, and in the cardiovascular system, Kv7.1, Kv7.4, and Kv7.5 are expressed in various combinations (Kubisch et al., 1999; Kharkovets et al., 2000; Loussouarn et al., 2006; Mackie and Byron, 2008).

The term M current comes from its depression by muscarinic receptor stimulation in sympathetic neurons (Brown and Adams, 1980; Constanti and Brown, 1981). After intense study, a wide spectrum of evidence indicates that this muscarinic action arises from the need of M channels for membrane PIP_2 to be functional (Zhang et al., 2003; Li et al., 2005; Suh et al., 2006) and the depletion of PIP_2 abundance in neurons by muscarinic agonist (Suh and Hille, 2002; Ford et al., 2003; Winks et al., 2005).

Correspondence to Mark S. Shapiro: shapirom@uthscsa.edu
C.C. Hernandez's present address is Dept. of Neurology, Vanderbilt University Medical Center, Nashville, TN 37232.

Abbreviations used in this paper: CHO, Chinese hamster ovary; FRET, fluorescence resonance energy transfer; oxo-M, oxotremorine-M; PI, phosphatidylinositol; WT, wild type.

The Rockefeller University Press $30.00
J. Gen. Physiol. Vol. 134 No. 5 437–448
www.jgp.org/cgi/doi/10.1085/jgp.200910313

Furthermore, cellular modeling has been used to quantify this system, yielding a biophysically satisfying framework that produces sufficient changes in PIP_2 abundance upon receptor stimulation to account for the observed depression of M current, given known rates of lipid enzymes, reasonable estimates of channel/PIP_2 affinities and plausible densities of PIP_2 molecules, and the signaling molecules relevant to this $G_{q/11}$-mediated system (Suh et al., 2004; Horowitz et al., 2005).

Single-channel analysis of Kv7.2–7.5 channels has revealed widely divergent activities of the channels in intact cells that can be ascribed to widely differential apparent affinities for PIP_2. Whereas Kv7.3 homomers have a very high saturating open probability (P_o) and high PIP_2 apparent affinity, Kv7.2 and Kv7.4 homomers display dramatically lower values, and Kv7.2/7.3 heteromers have intermediate values for saturating P_o and PIP_2 apparent affinity, as one might expect for heteromeric channels containing subunits with divergent affinities (Li et al., 2005). We have recently localized the region of the channel that accounts for divergent P_o and PIP_2 apparent affinity to a highly basic interhelical linker domain in the C terminus that is critical for PIP_2 interactions (Hernandez et al., 2008). Kv7.3 homomers in particular possess several unique properties. Although they display much greater apparent affinity for PIP_2 and saturating P_o than the others (Li et al., 2004, 2005; Hernandez et al., 2008) and their unitary conductance is also the highest, the whole-cell currents from heterologously expressed Kv7.3 homomers are at least 20-fold lower. We have suggested this aspect to be the result of a high fraction of wild-type (WT) Kv7.3 channels being dormant, a condition wholly reversed by a single point mutation in the inner pore at the 315 position from an alanine to a hydrophilic threonine or serine (Zaika et al., 2008), and for many of the experiments shown here, we exploit the high expression of Kv7.3 (A315T) channels, which we will refer to as $Kv7.3^T$ in this paper.

The widely divergent apparent affinity for PIP_2 of Kv7 channels predicts a corresponding divergence in sensitivity to stimulation of PLC-linked M_1 receptors because the degree of PIP_2 depletion should correlate with receptor stimulation, $G_{q/11}$ activation, and PLC activity. Thus, Kv7.3 is predicted to be relatively insensitive to muscarinic agonists, whereas Kv7.2 or Kv7.4 is predicted to be more sensitive. In addition, Kv7.2 mutants with decreased PIP_2 apparent affinity (Hernandez et al., 2008) should be more sensitive than WT channels, and increased tonic PIP_2 abundance should render channels less sensitive. In this study, we test these ideas on mammalian cells heterologously expressing various Kv7 channels and M_1 receptors and quantified agonist sensitivity as the dose–response relationship between muscarinic agonist concentration and Kv7-current inhibition. Furthermore, we modified a cellular model that simulates the $G_{q/11}$-mediated PLC signaling system, including PIP_2 metabolism and channel–PIP_2 interactions (Suh et al., 2004; Horowitz et al., 2005; Jensen et al., 2009), to model the relationship between receptor occupancy, PIP_2 affinity, and channel activity. The data and model are highly congruent, providing a satisfying biophysical basis for our observations.

MATERIALS AND METHODS

cDNA constructs

Human Kv7.2, Kv7.3, and Kv7.4 (GenBank/EMBL/DDBJ accession nos. AF110020, AF071478, and AF105202, respectively) were provided by D. McKinnon (Kv7.2; State University of New York at Stony Brook, Stony Brook, NY) and T. Jentsch (Kv7.3 and Kv7.4; Zentrum fur Molekulare Neurobiologie, Hamburg, Germany). Plasmids were subcloned into pcDNA3.1 using standard techniques. Mouse type 1α PI(4)P5-kinase (PIP 5-kinase) was provided by L. Pott (Ruhr-University, Bochum, Germany; Bender et al., 2002). Mutations were made by PCR using the QuikChange method (Agilent Technologies) and verified by sequencing. The Kv7.3 (A315T) mutant ($Kv7.3^T$) and all Kv7.2 mutants were made by site-directed mutagenesis using standard techniques and verified by dye-termination sequencing.

Cell culture and transfections

Chinese hamster ovary (CHO) cells were used for electrophysiological analysis as described previously (Gamper et al., 2005). Cells were grown in 100-mm tissue culture dishes (Falcon; BD) in Dulbecco's modified Eagle's medium with 10% heat-inactivated fetal bovine serum and 0.1% penicillin and streptomycin in a humidified incubator at 37°C (5% CO_2) and passaged every 3–4 d. Cells were discarded after ∼30 passages. For transfection, cells were plated onto poly-L-lysine–coated coverslip chips and transfected 24 h later with Polyfect reagent (QIAGEN) according to the instructions of the manufacturer. For electrophysiological experiments, cells were used 48–96 h after transfection. As a marker for successfully transfected cells, cDNA encoding green fluorescent protein was cotransfected together with the cDNAs of the genes of interest. We found that >95% of green fluorescing cells expressed Kv7 currents in control experiments.

Perforated-patch electrophysiology

Pipettes were pulled from borosilicate glass capillaries (1B150F-4; World Precision Instruments) using a Flaming/Brown micropipette puller (P-97; Sutter Instrument Co.) and had resistances of 1–2 MΩ when filled with internal solution and measured in standard bath solution. Membrane current was measured with pipette and membrane capacitance cancellation and was sampled at 5 ms and filtered at 1 kHz by an amplifier (EPC-9) and PULSE software (HEKA/Instrutech). In all experiments, the perforated-patch method of recording was used with 200–600 µg/ml amphotericin B in the pipette (Rae et al., 1991). Amphotericin was prepared as a stock solution as 60 mg/ml in DMSO. In these experiments, the access resistance was typically 10 MΩ 5–10 min after seal formation. Cells were placed in a 500-µl perfusion chamber through which solution flowed at 1–2 ml/min. Inflow to the chamber was by gravity from several reservoirs, selectable by activation of solenoid valves (Warner Scientific). Bath solution exchange was complete by <30 s. Experiments were performed at room temperature. The amplitude of the Kv7 current was usually defined as the holding current at 0 mV. In some cells, a more precise measurement was the XE991-sensitive current at the holding potential of 0 mV. CHO cells had negligible endogenous

macroscopic K^+ currents under our experimental conditions, and 10 µM XE991 completely blocked the K^+ current in Kv7-transfected CHO cells but had no effect on currents in nontransfected cells (Gamper et al., 2005). Dose–response data of channel current inhibition versus [oxotremorine-M] ([oxo-M]) were fit using Prism software (version 5.01; GraphPad Software, Inc.) for Windows by nonlinear regression using a Hill equation of the form

$$\text{Inhib} = \text{Inhib}_{max} \Big/ \left[1 + \left(\frac{x_{half}}{x}\right)^n\right],$$

where Inhib is the fractional inhibition of the Kv7 current, Inhib_{max} is the maximal inhibition, x is [oxo-M], x_{half} is the [oxo-M] at which inhibition = 50% of maximal inhibition, and n is the Hill coefficient, which we constrained to the value of one. All results are reported as mean ± SEM.

Solutions and materials

The external Ringer's solution used to record Kv7 currents in CHO cells contained 160 mM NaCl, 5 mM KCl, 2 mM $CaCl_2$, 1 mM $MgCl_2$, and 10 mM HEPES, pH 7.4, with NaOH. The pipette solution contained 160 mM KCl, 5 mM $MgCl_2$, 5 mM HEPES, and 10 mM EGTA, pH 7.4, with KOH and added amphotericin B (200–600 µg/ml). Reagents were obtained as follows: Dulbecco's modified Eagle's medium, fetal bovine serum, penicillin, and streptomycin were purchased from Invitrogen; amphotericin B was obtained from Sigma-Aldrich. XE991 was purchased from Tocris.

Modeling

A kinetic model was implemented in the Virtual Cell modeling and simulation framework (www.vcell.org). From within Virtual Cell, the model can be accessed by any user under Shared Models/bfalken/Hernandez Falkenburger Shapiro 2009. The rate constants and equations that constitute the model and initial values for the parameters are listed in Tables S1–S3. The model is a simplified adaptation of a model describing PIP_2 metabolism and Kv7.2/7.3 current by Hille and co-workers (Suh et al., 2004; Horowitz et al., 2005). Basal levels of PIP_2 were assumed to be 5,000 molecules/µm^2 based on the results of earlier modeling that well accounted for the onset and recovery rates of muscarinic suppression of Kv7.2/7.3 current (Suh et al., 2004) and from the calculated membrane-bound fraction of the PIP_2/IP_3-binding PH-PLCδ1 probe (Horowitz et al., 2005). Xu et al. (2003) used a value of 4,000/um^2 based on biochemical assays, but the exact number does not affect the conclusions drawn from the modeling (Fig. S1). Our model has only one invariant reaction rate for PIP_2 synthesis (syn) that lumps together activity of phosphatidylinositol (PI) 4-kinase and PIP 5-kinase. Syn prevents PIP_2 levels from falling to zero during application of muscarinic agonist (oxo-M) and mediates PIP_2 recovery after washout of agonist. The rates of receptor-independent steady-state PIP_2 degradation via PIP_2 phosphatase and basal PLC activities were lumped together (deg), whose value was chosen to keep PIP_2 levels stable at rest. The model simulates extracellular concentrations of oxo-M with a 10-s time constant for solution exchange, as determined by calibration experiments. For dose–response curves, oxo-M was modeled as applied for 100 s to ensure that steady state was reached as in the experiments. PLC is activated by muscarinic receptor agonist with an EC_{50} of 1.6 µM, a value chosen to allow significant PIP_2 changes over the entire oxo-M concentration range, which is the prerequisite to observe changes in Kv7 currents. The time constant for PLC activation was taken from fluorescence resonance energy transfer (FRET) measurements of PLC binding to $G_{\alpha q}$ (Jensen et al., 2009).

The amplitudes of Kv7 currents were implemented in two steps: PIP_2 binding to Kv7-channel subunits and generation of current by four Kv7 subunits. The K_A values for PIP_2 binding were 500 µm^{-2} Kv7.2 (WT), 75 µm^{-2} Kv7.3^T, 2,500 µm^{-2} Kv7.4, 10^6 µm^{-2} Kv7.2 (EEE), 75 µm^{-2} Kv7.2 (R463E), and 5,000 µm^{-2} Kv7.2 (R463Q). By analogy to the Hodgkin and Huxley term n^4, which combines the sensing state of four voltage sensors to determine the voltage-dependent open probability of the entire channel, we calculated the PIP_2-dependent open probability of the entire channel as the product of the PIP_2 saturation of the four channel subunits (Table S2). For the heteromeric channels consisting of WT or mutant Kv7.2 and 7.3 subunits, we assumed the channel tetramers to consist of two subunits of each type, which is sufficient for our purposes here. Because the PIP_2 saturation of Kv7.3^T subunits does not change much in response to oxo-M, the changes in Kv7.2/7.3 current are predominantly governed by the PIP_2 occupancy of the Kv7.2 subunits with an exponent of 2 and a K_A of 500. This implementation is thus similar to the earlier models (Suh et al., 2004; Horowitz et al., 2005), which used a K_A of 1,000 µm^{-2} for the entire Kv7.2/7.3 channel and an exponent of 1.8.

To get a sense of how the model works, we varied several parameters over a wide range and modeled the results (Fig. S1). We first modeled the effects of varying the K_A value of a subunit for PIP_2 on the dose–response relationship between muscarinic agonist and current inhibition for a homomeric channel (Fig. S1 A). When the model used values of K_A that varied from 75 to 2,400, two trends were evident. At the high end of the range (i.e., low-affinity subunits), a change in the K_A mostly results in a shift of the dose–response curve, with little impact on the maximum inhibition. However, at the low end of the range (i.e., high-affinity channels), a change in the K_A results in little displacement of the dose–response curve (quantified by the EC_{50}) but a big effect on the maximum inhibition. This can be understood in that maximum PLC activity does not reduce the PIP_2 abundance to zero but rather to a steady-state value that reflects the equilibrium between PLC-mediated consumption and PIP_2 synthesis. Thus, for the high-affinity channels whose overall n^4 affinity is near those steady-state values, the predominant effect of altering K_A in the low range is a change in maximal inhibition. However, for the low-affinity channels, the subunit occupancy at maximal [oxo-M], which is very low, will change little when K_A is altered in this high range. Thus, the predominant effect is a shift in the dose–response curve, as the amount of PLC activity needed for the same degree of PIP_2 unbinding changes accordingly. Fig. S1 B shows a similar analysis for a heteromeric channel in which two subunits are Kv7.2 and the other two have K_A values over the same wide range. One can see that the same principles apply but to a lesser extent, as expected from the invariant affinity of the Kv7.2 subunits that buffer the overall response.

PIP_2 abundance has been suggested to vary considerably among cell types. For a given cell, this value reflects the equilibrium between tonic PIP_2 synthesis by PI kinases (syn in our model) and degradation by tonic PIP_2 phosphatases and basal PLC activity (deg in our model). In Fig. S1 C, we model the effect on the dose–response curve for Kv7.2/3 heteromers of doubling the tonic PIP_2 abundance to 10,000 µm^{-2} by doubling the value of syn. In Fig. S1 D, we model the effect of the same maneuver on the relationship between [oxo-M] and PIP_2 abundance. It can be seen that there are some modest changes: the curve in Fig. S1 C is a little shifted to the left and the maximal inhibition is a little less, and the curve in Fig. S1 D has a steeper fall toward a steady-state value that is a little larger.

Online supplemental material

Tables S1, S2, and S3 present information on model parameters, the formulations describing the Kv7 currents, and initial values of the parameters, respectively. Fig. S1 characterizes the basic behavior of the model, as described in the Materials and methods section. Online supplemental material is available at http://www.jgp.org/cgi/content/full/jgp.200910313/DC1.

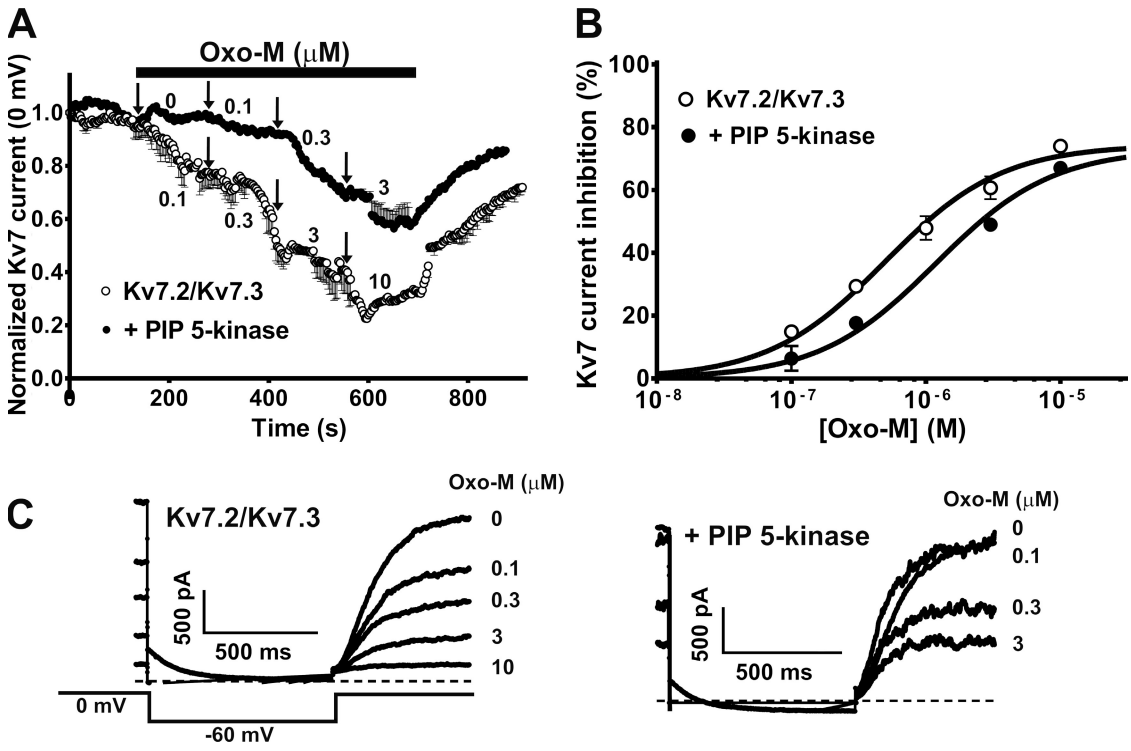

Figure 1. Agonist-induced Kv7.2/7.3-current suppression is reduced by overexpression of PIP 5-kinase. (A) Averaged time course of normalized current amplitude during sequential application of a range of concentrations of oxo-M to CHO cells coexpressing Kv7.2/7.3 channels and M_1 receptors, without (open circles) or together with PIP 5-kinase (closed circles). Times of applications of oxo-M at the given concentrations are indicated by the arrows. (B) Concentration dependence of current inhibition by oxo-M from cells expressing Kv7.2/7.3 alone (open circles) or together with PIP 5-kinase (closed circles). The lines represent the fits of experimental data by a Hill equation, with the values given in the text. Each point represents the mean ± SEM from $n = 5–7$ experiments. (C) Current waveforms before and after the application of a range of concentrations of oxo-M to CHO cells not coexpressing (left) or coexpressing PIP 5-kinase (right). The dashed line in the current traces is the zero current level, and the pulse protocol used is shown at the bottom in the left panel.

RESULTS

We studied CHO cells transfected with various Kv7 channels and M_1 muscarinic receptors under perforated-patch whole-cell voltage clamp. The inhibition of the current was quantified over a range of concentrations of the muscarinic agonist oxo-M. Our first experiments evaluated the muscarinic agonist sensitivity of WT Kv7.2/7.3 heteromers under control conditions and in cells in which tonic PIP_2 abundance was artificially increased. In control, the Kv7.2/7.3 current was inhibited by oxo-M in a concentration-dependent manner (Fig. 1, A and C) with an EC_{50} of 0.44 ± 0.08 μM ($n = 5–7$) and a maximal current inhibition of 74 ± 3% (Fig. 1 B, open circles). The EC_{50} value is comparable with that obtained previously in sympathetic neurons (0.30–0.68 μM; Bernheim et al., 1992; Haley et al., 2000; Winks et al., 2005), in which most M channels are thought to be Kv7.2/7.3 heteromers (Wang et al., 1998), but somewhat higher than that found in tsA-201 cells expressing the same channels and M_1 receptors (0.10–0.12 μM; Suh et al., 2004; Jensen et al., 2009). Likewise, the maximal inhibition is well within the range of that reported in sympathetic neurons (61–93%; Beech et al., 1991; Bernheim et al., 1992; Cruzblanca et al., 1998; Haley et al., 2000; Winks et al., 2005; Robbins et al., 2006; Zaika et al., 2007) but is on the low end of that reported in mammalian expression systems (79–95%; Selyanko et al., 2000; Shapiro et al., 2000; Gamper et al., 2003; Suh et al., 2004, 2006; Horowitz et al., 2005). We suspect that the precise values of both parameters will depend on the specific density of receptors or PLC molecules for each type of native, or heterologously transfected, cell.

PIP_2 is synthesized by sequential phosphorylation of PI by PI4- and PIP 5-kinases. Tonic PIP_2 levels have been experimentally increased by overexpression of PIP 5-kinase (Bender et al., 2002). In studies on M/Kv7 channels, the resulting effects were increases in unitary P_o at the single-channel level and current amplitude at the whole-cell level and a decrease in receptor-mediated suppression (Li et al., 2005; Winks et al., 2005; Suh et al., 2006). In general accord with those findings, we found overexpression of PIP 5-kinase to shift the oxo-M concentration dependence of Kv7.2/7.3-current suppression by threefold to higher concentrations (EC_{50} = 1.2 ± 0.08 μM, $n = 5–7$) but without any significant change in the maximal current inhibition (73 ± 4%; Fig. 1 B, open circles). These results are consistent with

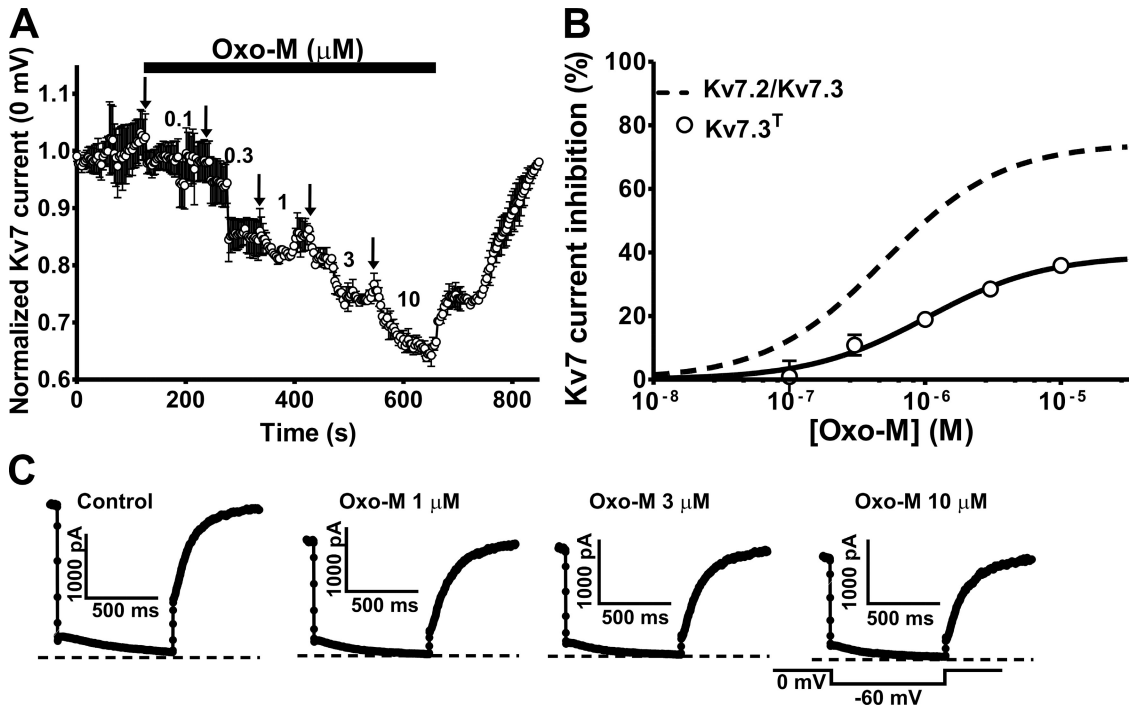

Figure 2. $Kv7.3^T$ currents display reduced sensitivity to muscarinic agonist. (A) Averaged time course of normalized $Kv7.3^T$-current amplitude during sequential application of a range of concentrations of oxo-M to CHO cells expressing $Kv7.3^T$ channels and M_1 receptors. Times of applications of oxo-M at the given concentrations are indicated by the arrows. (B) Concentration dependence of inhibition by oxo-M of $Kv7.3^T$ (open circles) and Kv7.2/7.3 (dashed line) current. The line represents the fit of the experimental data by a Hill equation with the values given in the text. Each point represents the mean ± SEM from $n = 5–7$ experiments. (C) $Kv7.3^T$-current waveforms before and after the application of oxo-M at the concentrations indicated. The dashed lines in the current traces are the zero current levels, and the pulse protocol is shown at the bottom in the right panel.

greater activity of molecules in the $G_{q/11}$ signaling pathway being required in the cells transfected with PIP 5-kinase relative to the activity required to reduce PIP_2 abundance in control cells to the level needed for a given amount of current inhibition. In our model, an increase in syn by 1.7-fold is required to produce our observed effect on the EC_{50} value, which is a little less than the twofold increase whose effect we modeled (Fig. S1, C and D). Our modeling also predicts a significant decrease in $Inhib_{max}$, which we did not observe. The relatively mild effects observed of PIP 5-kinase transfection, compared with previous studies, are probably caused either by less expression of PIP 5-kinase molecules than before or by a higher level of tonic PIP_2 abundance in the membrane in the present studies.

The muscarinic sensitivity of Kv7 channels correlates with their apparent affinity for PIP_2

Our previous work indicates the apparent affinity of PIP_2 for Kv7.3 homomers to be high and that of Kv7.2 or Kv7.4 homomers to be much lower, with Kv7.2/7.3 heteromers being intermediate (Li et al., 2005; Hernandez et al., 2008). To ask whether the sensitivity to muscarinic suppression of Kv7 channels correlates with differences in apparent PIP_2 affinity, we quantified the dose–response relationship of muscarinic agonist and current suppression for Kv7.3 and Kv7.4 homomers. Many laboratories report only tiny Kv7.3 homomeric currents in heterologous systems (Etxeberria et al., 2004; Schenzer et al., 2005; Zaika et al., 2008), which would preclude the dose–response analysis desired here. Thus, for the Kv7.3 experiments, we used the A315T pore mutant, which displays large whole-cell currents that enable such analysis, with no changes in the unitary P_o of the channel at saturating voltages, indicating that the A315T mutation does not alter the high PIP_2 apparent affinity of Kv7.3 subunits (Zaika et al., 2008). We will call this mutant $Kv7.3^T$ in this paper. Compared with Kv7.2/7.3 heteromers, the most dramatic difference for $Kv7.3^T$ homomers was the strongly reduced maximal inhibition of the current at high oxo-M concentrations. Thus, at 10 μM oxo-M, the $Kv7.3^T$ current was suppressed by only 39 ± 3% ($n = 5–7$; Fig. 2, A and C), whereas there was only a slight shift of the oxo-M dose–response curve to higher concentrations (EC_{50} = 1.0 ± 0.76 μM, $n = 5–7$; Fig. 2 B). As discussed below, these data suggest that at supramaximal concentrations of muscarinic agonist, the equilibrium between PLC-mediated consumption and synthesis of PIP_2 results in a PIP_2 abundance at which most high-affinity $Kv7.3^T$ channels are still bound by PIP_2 molecules. This hypothesis is further explored in the modeling to follow.

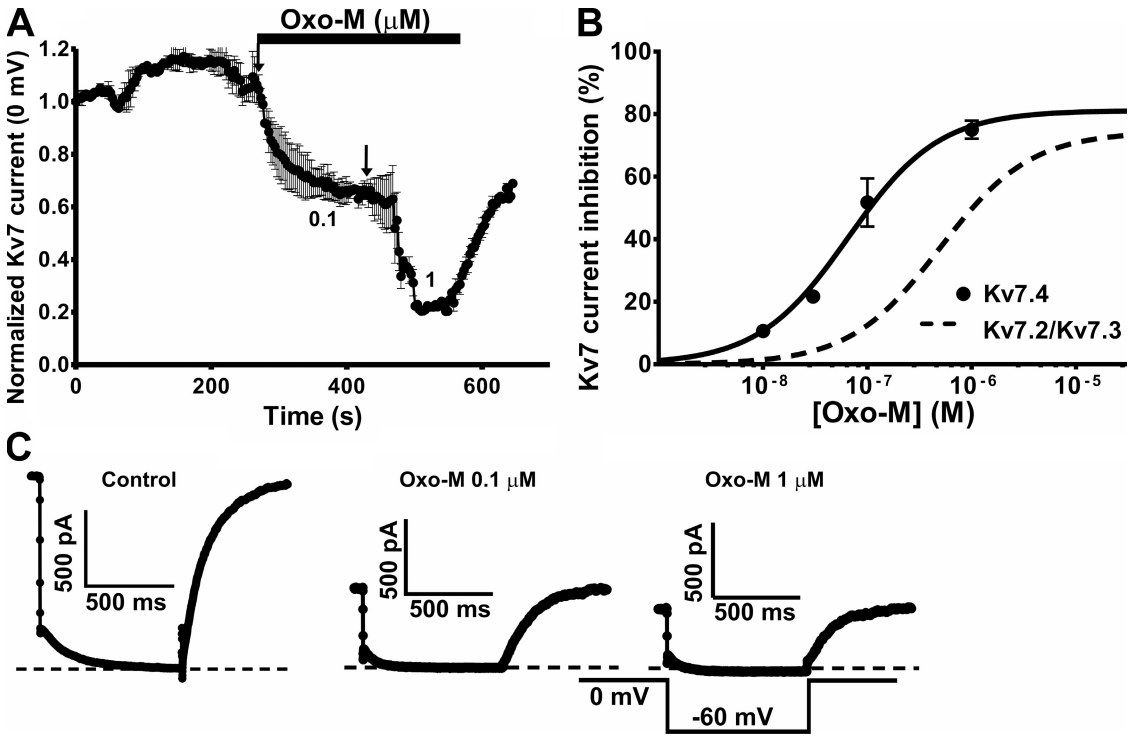

Figure 3. Kv7.4 channels are more sensitive to suppression by muscarinic stimulation. (A) Averaged time course of normalized Kv7.4-current amplitude during sequential application of a range of concentrations of oxo-M to CHO cells expressing Kv7.4 channels and M_1 receptors. Times of applications of oxo-M at the given concentrations are indicated by the arrows. (B) Concentration dependence of inhibition by oxo-M of the Kv7.4 (closed circles) and Kv7.2/7.3 (dashed line) currents. The line represents the fit of experimental data by a Hill equation, with the values given in the text. Each point represents the mean ± SEM from $n = 3$–4 experiments. (C) Kv7.4 current waveforms before and after the application of oxo-M at the concentrations indicated. The dashed lines in the current traces are the zero current levels, and the pulse protocol is shown at the bottom in the right panel.

In contrast, lower affinity Kv7.4 homomers displayed an inhibition of ∼75% at 1 μM oxo-M (Fig. 3, A and C), a concentration that produced only ∼19% inhibition of the Kv7.3^T current (Fig. 2, B and C), and ∼48% inhibition of the Kv7.2/7.3 current (Fig. 3 B, dashed line). Analyzed over a wide range of agonist concentrations, the dose dependence of Kv7.4-current suppression by oxo-M was shifted to lower concentrations by approximately sevenfold (EC_{50} = 66 ± 8 nM, n = 3–4) compared with Kv7.2/7.3 channels and by 15-fold compared with Kv7.3^T channels. Interestingly, there was no significant difference from Kv7.2/7.3 channels with regard to maximal suppression (81 ± 6%; Fig. 3 B). Thus, the activity of molecules in the $G_{q/11}$ signaling pathway required to reduce PIP_2 levels enough to cause unbinding of PIP_2 from low apparent affinity Kv7.4 channels must be significantly less than the activity required to cause PIP_2 unbinding from higher affinity Kv7.2/7.3 channels or highest affinity Kv7.3^T channels. These ideas are also tested in our modeling below.

Putative PIP_2-interacting residues within an interhelical domain in the C terminus control muscarinic sensitivity

We have localized the primary binding site of PIP_2 to M channels to a C-terminal domain that consists of a cluster of conserved basic amino acids within a seven–β-sheet barrel motif common to other PIP_2-binding domains (Hernandez et al., 2008). Interestingly, that study found mutation of two conserved basic residues in Kv7.2 (R463 and R467) within the cationic cluster to display opposite effects on PIP_2 apparent affinity that depended on the nature (charge reversal vs. charge neutralization) of the substituted residues, observations explained by molecular modeling and docking simulations (Hernandez et al., 2008). To ask whether muscarinic agonist sensitivity correlates with the observed changes in PIP_2 apparent affinity of one such Kv7.2 mutant pair, we studied R463E and R463Q, which were previously shown to have a much higher and lower apparent affinity for PIP_2, respectively (Hernandez et al., 2008). However, because cells transfected with those mutants display only small whole-cell currents (Hernandez et al., 2008), we studied the oxo-M concentration dependence for inhibition of R463E and R463Q mutant subunits coexpressed with Kv7.3^T (Fig. 4). For Kv7.2 (R463E)/7.3^T, the muscarinic sensitivity was sharply reduced, manifested by a reduction in the maximal inhibition of the current to 27 ± 3% and a slight shift of the EC_{50} to higher concentrations (0.58 ± 0.07 μM, n = 3–4), compared with Kv7.2/7.3 (Fig. 4, A and B). In contrast, mutation of R463 to the

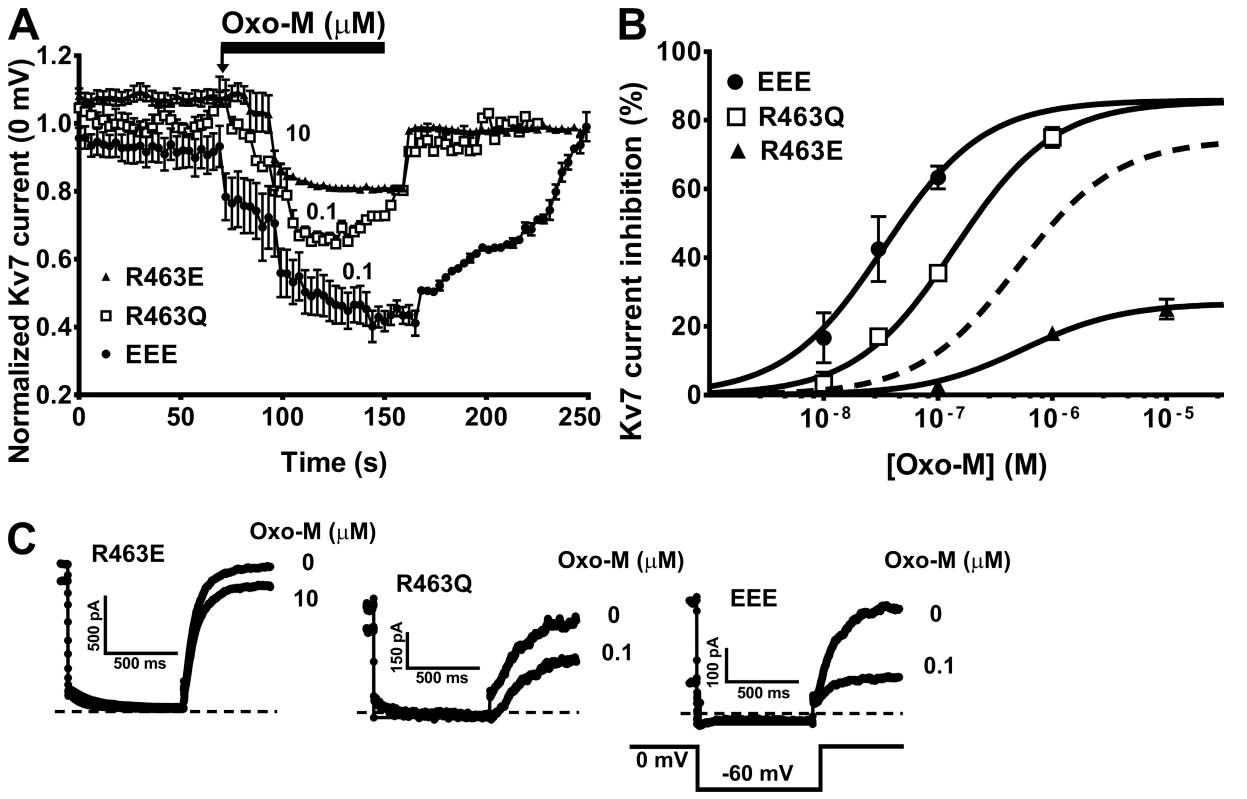

Figure 4. Altered PIP_2 sensitivity of Kv7.2 mutant subunits confers differential sensitivity to muscarinic stimulation. (A) Averaged time course of normalized current amplitude during an application of a single concentration of oxo-M to CHO cells expressing M_1 receptors together with Kv7.2 (R463E)/7.3^T channels (closed triangles), Kv7.2 (R463Q)/7.3^T channels (open squares), or Kv7.2 (EEE)/7.3^T channels (closed circles). The time of application of oxo-M at the given concentration is indicated by the arrow. (B) Concentration dependence of inhibition by oxo-M of Kv7.2 (R463E)/7.3^T (closed triangles), Kv7.2 (R463Q)/7.3^T (open squares), Kv7.2 (EEE)/7.3^T (closed circles), or Kv7.2/7.3 (dashed line) current. The line represents the fit of experimental data by a Hill equation, with the values given in the text. Each point represents the mean ± SEM from n = 3–4 experiments. (C) Kv7.2 mutant current waveforms before and after the application of oxo-M at the concentrations indicated. The dashed lines in the current traces are the zero current levels, and the pulse protocol is shown at the bottom in the right panel.

noncharged glutamine shifted the dose dependence of Kv7.2 (R463Q)/7.3^T channels to lower concentrations by fourfold (Fig. 4, A and B). For those heteromers, the EC_{50} was reduced to 0.12 ± 0.08 μM with a maximal inhibition of 79 ± 6% (n = 3–4). We then investigated the effect on muscarinic sensitivity of incorporation into the channels of the Kv7.2 K452E/R459E/R461E triple mutant (EEE), in which the charges of three conserved basic residues important for PIP_2 interactions in the putative PIP_2-binding domain are simultaneously reversed, causing a profound reduction in single-channel open probability and presumed PIP_2 affinity (Hernandez et al., 2008). For the Kv7.2 (EEE)/7.3^T heteromer, the muscarinic sensitivity was indeed strongly increased, with the EC_{50} reduced to 32 ± 4 nM (n = 3–4) and a maximal current inhibition of 83 ± 3% (n = 3–4; Fig. 4 B, circles). This shift of the oxo-M dose–response relation, as measured by the change in EC_{50}, represents a 14-fold and 18-fold increase in muscarinic sensitivity relative to the higher affinity Kv7.2/7.3 and Kv7.2 (R463E)/7.3^T channels, respectively, and even a fourfold increase when compared with Kv7.2 (R463Q)/7.3^T channels (Fig. 4). Thus, the currents from Kv7.2 (EEE)/7.3^T mutant channels were inhibited by ∼60% at 0.1 μM oxo-M, a concentration that produced an inhibition of Kv7.2 (R463Q)/7.3^T channels of only ∼30% (Fig. 4 C). In summary, our results suggest that sensitivity to muscarinic agonist via $G_{q/11}$-coupled M_1 receptors, PLC activity, and consumption of PIP_2 correlates well with apparent PIP_2 affinity across the family of homomeric and heteromeric M-type channels both for WT Kv7 variants and for the Kv7.2 mutants. They also suggest that the PIP_2 affinity of one type of subunit in a heteromer has strong effects on the overall PIP_2 affinity and subsequent muscarinic sensitivity of the overall tetrameric channel. Thus, PIP_2 binding to all subunits in the tetramer is likely to be required for the channel to be activatable by voltage.

A cellular model of $G_{q/11}$ signaling provides a biophysical model of our observations

We used a simplified version (Fig. 5 A) of a more comprehensive kinetic model developed previously (Suh et al., 2004) to show that our experimental findings can be explained by the basic principles of $G_{q/11}$ signaling

and channels regulated by PIP_2 abundance, which we assume to tonically be 5,000 molecules/μm^2 of plasma membrane.. In our model here, Kv7.2, 7.3, and 7.4 subunits or mutant Kv7.2 subunits possess distinct affinities for PIP_2, quantified as the K_A for PIP_2 binding, which was empirically determined to best fit the data. For Kv7.2–7.4, the K_A values were 500, 75, and 2,500, and for the Kv7.2 mutants R463E, R463Q, and the EEE mutant, they were 75, 5,000, and 10^6, respectively. The model supposes binding of one PIP_2 to one Kv7 subunit. Because each channel is composed of four subunits, the current of a Kv7 channel is proportional to the product of the fractional PIP_2 saturation of four subunits (see Materials and methods and Table S2). We assumed heteromeric Kv7.2/7.3 channels to consist of two Kv7.2 (WT or mutant) and two Kv7.3 subunits, which is reasonable for our purposes here. For homomeric channels, current was modeled as being proportional to the fourth power of PIP_2-bound subunits. This implementation differs from the model by Suh et al. (2004) in which PIP_2 bound to a channel particle instead of to a subunit particle, which did not allow "mixing" of Kv7.2 and 7.3 subunits to form a heteromeric channel. Thus, we first determined the affinity of homomeric channels to determine the affinity of each type of WT subunit and then adjusted the affinity of WT or mutant Kv7.2 subunits to reproduce the dose–response relationships observed experimentally with Kv7.2/7.3 heteromers. Our model reflects the affinity of PIP_2 for Kv7.2, 7.3, and 7.4 subunits to be intermediate, high, and low, respectively, and the R463E and R463Q mutants of Kv7.2 to give that subunit high (similar to Kv7.3) and low (similar to Kv7.4) affinities for PIP_2, respectively. Finally, in our model, the EEE mutant possesses a profoundly low PIP_2 affinity, which is in accord with the very low affinity predicted in our earlier docking simulations and seen in single-channel patches (Hernandez et al., 2008).

The first important observation is the relationship between PIP_2 density and concentration of receptor agonist (Fig. 5 B). The activation of PLC by oxo-M was informed by measurements of muscarinic agonist–induced changes in FRET between $G\alpha_q$ and PLC (Jensen et al., 2009) and adjusted to produce significant changes in PIP_2 density over the entire range of oxo-M concentrations in which current inhibition was observed. Steady-state PIP_2 density reflects the equilibrium between consumption by PLC and synthesis by PI kinases, with half-maximal PIP_2 reduction at ~0.2 µM oxo-M (Fig. 5 B). PIP_2 synthesis during oxo-M application is greater than zero (and in fact stimulated as compared with baseline values; Gamper et al. 2004). PLC activity saturates at a finite value, as there are a finite number of PLC molecules that can be activated. As a consequence, there is a defined, nonzero minimum level for PIP_2 in the presence of maximal oxo-M concentrations (~500 μm^{-2} in Fig. 5 B). As a consequence, the inhibition of all Kv7 channels will saturate at high [oxo-M] (Fig. 5 C). $Inhib_{max}$ is predicted to diverge between Kv7 channels, depending on their affinity for PIP_2. Low-affinity channels will have lost virtually all their bound PIP_2 molecules at minimal PIP_2 densities, whereas a substantial proportion of high-affinity channels will retain their bound PIP_2. The small maximum inhibition of Kv7.3 current at supramaximal oxo-M is thus explained by the fact that, because of their high PIP_2 affinity, they retain much of their bound PIP_2 even at maximal PLC activity (Fig. 5 C, dashed line). Another consequence of the high affinity of Kv7.3 for PIP_2 is that the channel is relatively PIP_2 saturated at rest, and the predicted relationship between PIP_2 abundance and Kv7.3 current is relatively flat at resting PIP_2 densities (Fig. 5 D, dashed line). Low concentrations of oxo-M are therefore predicted to have virtually no effect on Kv7.3 current, in accord with the data. Conversely, Kv7.4 has a low affinity for PIP_2, and the PIP_2 concentration curve for Kv7.4 is relatively steep in the area of resting PIP_2 (Fig. 5 D, dotted line). This results in strong current reduction even by small changes of PIP_2 abundance and augmented inhibition at saturating [oxo-M]. Current inhibition thus requires only little oxo-M, low activation of receptors, $G_{q/11}$, and PLC, explaining the left-shifted concentration curve as compared with Kv7.2/7.3 channels (Fig. 5 C, dotted line). The comparison between values for EC_{50} and maximal inhibition for the data and model values for Kv7.3, 7.4, and 7.2/7.3 channels are nicely in accord (Table I), providing satisfying support for our thinking.

The next set of modeling has to do with the behavior of the Kv7.2 mutants. Again, we assumed a 1:1 stoichiometry in the channel tetramers made from coexpressed Kv7.2 mutant subunits and Kv7.3 subunits, with current proportional to the sequential product of four PIP_2-bound subunits. We assume that the changes in muscarinic sensitivity for the higher or lower PIP_2 affinity Kv7.2 mutants studied here can be ascribed to the same biophysical principles as for the WT channels. In the model, the best fit for the data from Kv7.2 (R463E) and (R463Q) subunits were with PIP_2 affinities similar to that of Kv7.3 or Kv7.4 subunits, respectively, and the PIP_2 affinity needed for the Kv7.2 (EEE) mutant had to be made extremely low. Thus, for Kv7.2 (R463E)/Kv7.3 channels, the relationship between current inhibition and [oxo-M] is predicted to be flat at low [oxo-M] with relatively low inhibition at saturating [oxo-M], which is in accord with the data, like that of Kv7.3 homomers. Conversely, for Kv7.2 (R463Q)/7.3 channels, the relationship between current inhibition and [oxo-M] is predicted to be relatively steep at low [oxo-M], resulting in strong current reduction by small changes in PIP_2 abundance and augmented inhibition at saturating [oxo-M], all similar to the response of Kv7.4 homomers. In the model, the oxo-M sensitivity of Kv7.2 (EEE)/Kv7.3 channels is only slightly greater than that for Kv7.2

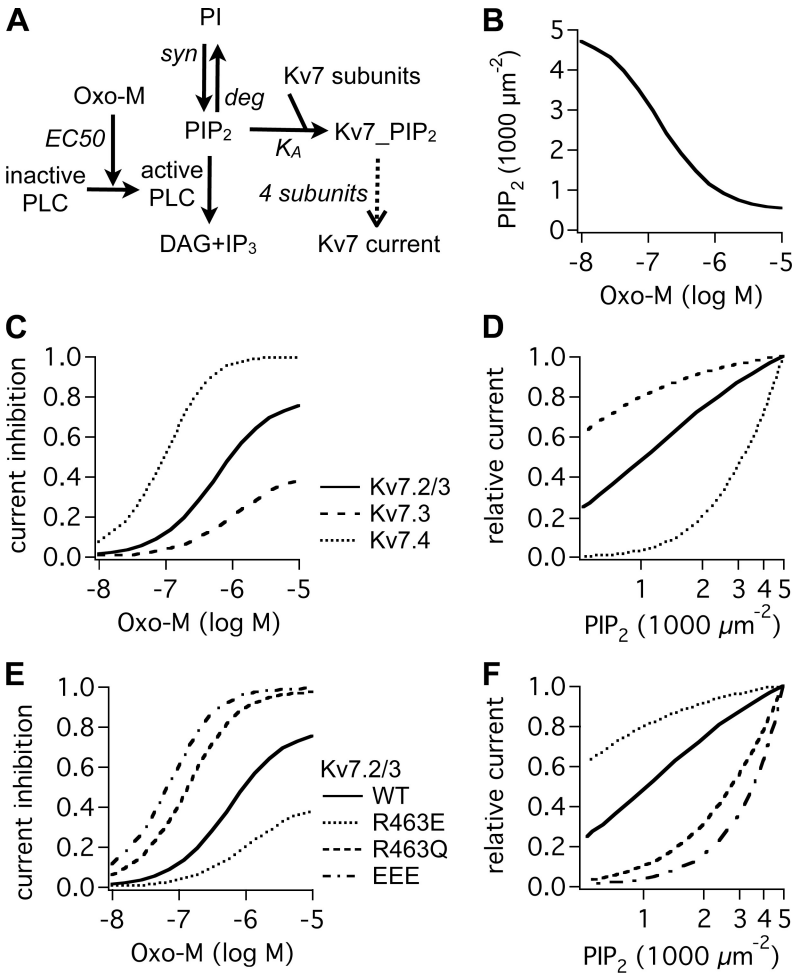

Figure 5. A kinetic model reproduces the experimental findings. (A) Model reactions. Oxo-M activates PLC, which hydrolyzes PIP_2. Kv7 subunits bind to PIP_2, which allows Kv7 current. Each Kv7 channel is formed by a set of four Kv7 subunits, which can differ in their PIP_2 affinity in the case of heteromers or are identical in the case of homomers. K_A values for Kv7 subunits are 500 μm^{-2} Kv7.2 (WT), 75 μm^{-2} Kv7.3 (assumed to be the same as $Kv7.3^T$), 2,500 μm^{-2} Kv7.4, 10^6 μm^{-2} Kv7.2 (EEE), 75 μm^{-2} Kv7.2 (R463E), and 5,000 μm^{-2} Kv7.2 (R463Q). Also see Tables S1–S3. DAG, diacylglycerol. (B–F) Model outputs. (B) Steady-state levels of PIP_2 reached under a range of concentrations of oxo-M. (C and E) Maximum current inhibition over a range of concentrations of oxo-M. (D and F) Dependence of current amplitudes (relative to baseline) on PIP_2 levels.

(R463Q)/Kv7.3 channels, but this is actually predicted by the dominance of PIP_2 binding to the Kv7.3 subunits in the tetramer and is again very similar to the data. Note that at intermediate oxo-M concentrations for both the data and the model, the difference in the response of Kv7.2 (R463Q)/Kv7.3 and Kv7.2 (EEE)/Kv7.3 channels is most significant. In the Discussion, we compare the current experimental and model data with our previous molecular docking simulations.

TABLE I

Comparison of data and model values for muscarinic inhibition of the indicated Kv7 channels by oxo-M

Channel	Data		Model	
	EC_{50}	$Inhib_{max}$	EC_{50}	$Inhib_{max}$
	μM	%	*μM*	%
Kv7.2wt/7.3wt	0.44 ± 0.08	74 ± 3	0.54	81
$Kv7.3^T$	1.0 ± 0.76	39 ± 3	1.05	41
Kv7.4wt	0.066 ± 0.008	81 ± 6	0.10	99
Kv7.2 (R463E)/7.3^T	0.58 ± 0.07	27 ± 3	1.05	41
Kv7.2 (R463Q)/7.3^T	0.12 ± 0.08	79 ± 6	0.13	97
Kv7.2 (EEE)/7.3^T	0.032 ± 0.004	83 ± 3	0.07	99

The values for both data and model were taken from Hill equation fits in both cases.

DISCUSSION

Two related types of single-channel experiments have suggested that the family of Kv7 channels possesses divergent apparent affinities for PIP_2. The first are cell-attached patch recordings in which channel P_o at saturating voltages varied widely, consistent with the tonic PIP_2 abundance supporting a divergent level of channel opening. The second are inside-out patch data in which P_o measured over a wide range of concentrations of a water-soluble PIP_2 analogue revealed a parallel differential PIP_2 apparent affinity (Hernandez et al., 2008). These results predicted a corresponding divergent dose–response relationship between PLC-linked receptor agonist and Kv7-channel inhibition. That prediction was verified here. A main result of this work is that the effect of alterations in PIP_2 affinity on the sensitivity of the channels to muscarinic agonist depends on whether the channels have a relatively low or high apparent affinity for PIP_2. For the former, reductions in PIP_2 affinity do not much affect the $Inhib_{max}$ because it is already quite high but rather shift the dose–response relation of [oxo-M] versus inhibition to lower concentrations. Conversely, for the latter, reductions in affinity do not much change the EC_{50} of the dose–response relation, but rather the

large effect is an increase in $Inhib_{max}$. Thus, the current from Kv7 channels does not generally go to zero upon maximal stimulation of M_1 receptors, but rather $Inhib_{max}$ depends on the equilibrium between PLC-mediated hydrolysis and PIP_2 synthesis and the affinity of the particular channel. All of these phenomena are well simulated by our model incorporating PIP_2 metabolism, receptor-mediated PLC activation, and channels regulated by PIP_2 binding with quantifiable affinities. What adds impact to our results is that agonist-dependent PIP_2 depletion or creation is highly receptor and cell dependent. Thus, PIP_2 binding/unbinding is hypothesized to often occur not via PIP_2 depletion but rather via alteration of the PIP_2 affinity of PIP_2-regulated channels by myriad signaling molecules (Gβγ, Ca^{2+}/calmodulin, pH, Na^+, PKC, PKA, etc.; Gamper and Shapiro, 2007). Therefore, the changes of PIP_2 affinity by mutagenesis or change of subunit composition in these experiments somewhat mimic this physiological mechanism of lipid signaling. For example, whereas Kv7.3 homomers are only slightly inhibited at maximal depletion of PIP_2 by PLC, a reduction in the channel's affinity for PIP_2 will put its K_A in the range where such physiological depletions will have a much stronger effect on the currents. In addition, the strong subunit dependence of muscarinic agonist sensitivity predicts that transcriptional control of subunit expression in distinct regions of the nervous system will have profound consequences for muscarinic receptor control over neuronal excitability.

The cellular modeling makes predictions for the values of EC_{50} and $Inhib_{max}$ for muscarinic suppression of the Kv7 subunits that we studied. Those predicted and experimental values are compared in Table I. For clarity, we will use Kv7.2/7.3 heteromers as the baseline to compare with the others in this discussion. Several trends are clearly in accord between the two sets of values. First, they both show high-affinity channels ($Kv7.3^T$ and Kv7.2 (R463E)/$Kv7.3^T$) to have sharply reduced $Inhib_{max}$ but only slightly increased EC_{50} values. Second, they both show low-affinity channels (Kv7.4, Kv7.2 (R463Q)/$Kv7.3^T$, and Kv7.2 (EEE)/$Kv7.3^T$) to manifest strongly decreased EC_{50} values. The model also predicts the significant current remaining after maximal receptor stimulation for intermediate affinity channels, which is in accord with the experimental observations. However, a clear discrepancy is the near complete elimination of the current by low-affinity channels predicted by the model, which we did not observe in the data. An explanation may be the existence of "protected" pools of PIP_2 (perhaps sequestered by MARCKS [myristoylated alanine-rich C-kinase substrate] proteins or other PIP_2-sequestering moieties; Gambhir et al., 2004; McLaughlin et al., 2005; Milosevic et al., 2005) that cannot be consumed by PLC, preventing Kv7-channel activity from ever going to zero. Alternatively, the CHO cells that we use for our heterologous expression system may be endowed with receptor-mediated stimulation of PIP_2 synthesis, as has been demonstrated in neurons (Xu et al., 2003; Gamper et al., 2004; Loew, 2007). Lastly, there may be feedback acceleration of the activity of PI kinases tied to PIP_2 levels (Hilgemann et al., 2001). Both of these factors may prevent PIP_2 levels from being as depleted as in our modeling, which does not incorporate any feedback alteration in the rate of PIP_2 synthesis. We cannot know for sure whether the stoichiometry of subunits in the coexpression of the Kv7.2 mutants with $Kv7.3^T$ is as nearly 1:1 as we assume, which would bias the data if more $Kv7.3^T$ subunits were in the tetramers. However, this caveat does not apply for Kv7.4 homomers, which also manifested a more complete suppression of the current in the model than in the data.

We should also comment on the variance in dose–response relationships described in the literature for muscarinic suppression of M current and of PIP_2 depletion. Steady-state PIP_2 densities achieved at various concentrations of $G_{q/11}$-coupled receptor agonists are expected to be very much dependent on the experimental paradigm and cell type used; for example, whether the receptors are endogenous or heterologously expressed or whether PI kinases are stimulated by receptor stimulation. Jensen et al. (2009) recently determined an oxo-M dose–response curve for PIP_2 densities using the PH-PLCδ1 FRET probe in which the EC_{50} for oxo-M–mediated depletion of PIP_2 was found to be ∼10-fold lower than in the present modeling results (Fig. 5 B). Although PH-PLCδ1 probe expression can affect phosphoinositide levels and metabolism (Xu et al., 2003; Gamper et al., 2004), the oxo-M dose–response curve for Kv7.2/7.3 inhibition was also shifted by about fourfold in cells not expressing the probe. We suspect the differences could result from lower levels of endogenous G proteins or PLC molecules in CHO cells as compared with tsA-201 cells or reflect a higher activity of PI kinases. In addition, much work indicates receptor-mediated stimulation of PI-kinases, which is concurrent with activation of PLC (Zhao et al., 2001; Koizumi et al., 2002; Rajebhosale et al., 2003; Xu et al., 2003; Gamper et al., 2004; Winks et al., 2005; Zheng et al., 2005; Balla and Balla, 2006). Thus, differential stimulation of PI-kinases across cell types could easily account for the differences seen in agonist sensitivity and efficacy toward ion channel targets.

In this study, the K_A values for binding of PIP_2 to Kv7.2, 7.3, 7.4, 7.2 (R463E), 7.2 (R463Q), and 7.2 (EEE) subunits were modeled to be 500, 75, 2,500, 75, 5,000, and 10^6, respectively. Using the classical relationship between equilibrium constant and free energy of $\Delta G = -RTln(K_A)$, those affinities correspond to differences in free energy relative to Kv7.2 of 4.7 (Kv7.3), −4.0 (Kv7.4), 4.7 (Kv7.2 R463E), −5.7 (Kv7.2 R463Q), and −18.9 (Kv7.2 EEE) kJ/M. In our docking simulations between the channels' putative PIP_2-binding domains and the PIP_2 analogue, GPMI-P_2, the differences in affinity energies

were found, relative to Kv7.2, to be 2.2 (Kv7.3), 3.8 (Kv7.2 R463E), −5.7 (Kv7.2 R463Q), and −11.2 (Kv7.2 EEE) kJ/M (docking with Kv7.4 was not modeled; Hernandez et al., 2008). Although there are quantitative differences between the present modeling results and the previous docking simulations, there is qualitative agreement that lends credence to the docking simulations and adds to an internally consistent body of data and modeling across single-channel patches, receptor-mediated modulation in intact cells, homology/docking modeling, and the model simulations. Clearly, the next step will be to perform biochemical affinity measurements for the PIP_2-binding domains of the various M-type channels to test whether our conclusions from signaling cascades translate into quantitative measurements of physical molecular interactions.

We thank P. Reed for expert technical assistance and B. Hille for discussions.

This work was supported by National Institutes of Health grant R01 NS043394 (to M.S. Shapiro), American Heart Association grant-in-aid 0755071Y (to M.S. Shapiro), and the Human Frontier Science Program (to B. Falkenburger).

Lawrence G. Palmer served as editor.

Submitted: 7 August 2009
Accepted: 8 October 2009

REFERENCES

Balla, A., and T. Balla. 2006. Phosphatidylinositol 4-kinases: old enzymes with emerging functions. *Trends Cell Biol.* 16:351–361. doi:10.1016/j.tcb.2006.05.003

Beech, D.J., L. Bernheim, A. Mathie, and B. Hille. 1991. Intracellular Ca^{2+} buffers disrupt muscarinic suppression of Ca^{2+} current and M current in rat sympathetic neurons. *Proc. Natl. Acad. Sci. USA.* 88:652–656. doi:10.1073/pnas.88.2.652

Bender, K., M.C. Wellner-Kienitz, and L. Pott. 2002. Transfection of a phosphatidyl-4-phosphate 5-kinase gene into rat atrial myocytes removes inhibition of GIRK current by endothelin and alpha-adrenergic agonists. *FEBS Lett.* 529:356–360. doi:10.1016/S0014-5793(02)03426-9

Bernheim, L., A. Mathie, and B. Hille. 1992. Characterization of muscarinic receptor subtypes inhibiting Ca^{2+} current and M current in rat sympathetic neurons. *Proc. Natl. Acad. Sci. USA.* 89:9544–9548. doi:10.1073/pnas.89.20.9544

Brown, D.A., and P.R. Adams. 1980. Muscarinic suppression of a novel voltage-sensitive K^+ current in a vertebrate neurone. *Nature.* 283:673–676. doi:10.1038/283673a0

Constanti, A., and D.A. Brown. 1981. M-Currents in voltage-clamped mammalian sympathetic neurones. *Neurosci. Lett.* 24:289–294. doi:10.1016/0304-3940(81)90173-7

Cooper, E.C., E. Harrington, Y.N. Jan, and L.Y. Jan. 2001. M channel KCNQ2 subunits are localized to key sites for control of neuronal network oscillations and synchronization in mouse brain. *J. Neurosci.* 21:9529–9540.

Cruzblanca, H., D.S. Koh, and B. Hille. 1998. Bradykinin inhibits M current via phospholipase C and Ca^{2+} release from IP_3-sensitive Ca^{2+} stores in rat sympathetic neurons. *Proc. Natl. Acad. Sci. USA.* 95:7151–7156. doi:10.1073/pnas.95.12.7151

Delmas, P., and D.A. Brown. 2005. Pathways modulating neural KCNQ/M (Kv7) potassium channels. *Nat. Rev. Neurosci.* 6:850–862. doi:10.1038/nrn1785

Etxeberria, A., I. Santana-Castro, M.P. Regalado, P. Aivar, and A. Villarroel. 2004. Three mechanisms underlie KCNQ2/3 heteromeric potassium M-channel potentiation. *J. Neurosci.* 24:9146–9152. doi:10.1523/JNEUROSCI.3194-04.2004

Ford, C.P., P.L. Stemkowski, P.E. Light, and P.A. Smith. 2003. Experiments to test the role of phosphatidylinositol 4,5-bisphosphate in neurotransmitter-induced M-channel closure in bullfrog sympathetic neurons. *J. Neurosci.* 23:4931–4941.

Gambhir, A., G. Hangyás-Mihályné, I. Zaitseva, D.S. Cafiso, J. Wang, D. Murray, S.N. Pentyala, S.O. Smith, and S. McLaughlin. 2004. Electrostatic sequestration of PIP_2 on phospholipid membranes by basic/aromatic regions of proteins. *Biophys. J.* 86:2188–2207. doi:10.1016/S0006-3495(04)74278-2

Gamper, N., and M.S. Shapiro. 2007. Regulation of ion transport proteins by membrane phosphoinositides. *Nat. Rev. Neurosci.* 8:921–934. doi:10.1038/nrn2257

Gamper, N., J.D. Stockand, and M.S. Shapiro. 2003. Subunit-specific modulation of KCNQ potassium channels by Src tyrosine kinase. *J. Neurosci.* 23:84–95.

Gamper, N., V. Reznikov, Y. Yamada, J. Yang, and M.S. Shapiro. 2004. Phosphatidylinositol [correction] 4,5-bisphosphate signals underlie receptor-specific $G_{q/11}$-mediated modulation of N-type Ca^{2+} channels. *J. Neurosci.* 24:10980–10992. doi:10.1523/JNEUROSCI.3869-04.2004

Gamper, N., J.D. Stockand, and M.S. Shapiro. 2005. The use of Chinese hamster ovary (CHO) cells in the study of ion channels. *J. Pharmacol. Toxicol. Methods.* 51:177–185. doi:10.1016/j.vascn.2004.08.008

Haley, J.E., F.C. Abogadie, J.M. Fernandez-Fernandez, M. Dayrell, Y. Vallis, N.J. Buckley, and D.A. Brown. 2000. Bradykinin, but not muscarinic, inhibition of M-current in rat sympathetic ganglion neurons involves phospholipase C-beta 4. *J. Neurosci.* 20:RC105.

Hernandez, C.C., O. Zaika, and M.S. Shapiro. 2008. A carboxy-terminal inter-helix linker as the site of phosphatidylinositol 4,5-bisphosphate action on Kv7 (M-type) K^+ channels. *J. Gen. Physiol.* 132:361–381. doi:10.1085/jgp.200810007

Hilgemann, D.W., S. Feng, and C. Nasuhoglu. 2001. The complex and intriguing lives of PIP_2 with ion channels and transporters. *Sci. STKE.* doi:10.1126/stke.2001.111.re19

Horowitz, L.F., W. Hirdes, B.C. Suh, D.W. Hilgemann, K. Mackie, and B. Hille. 2005. Phospholipase C in living cells: activation, inhibition, Ca^{2+} requirement, and regulation of M current. *J. Gen. Physiol.* 126:243–262. doi:10.1085/jgp.200509309

Jensen, J.B., J.S. Lyssand, C. Hague, and B. Hille. 2009. Fluorescence changes reveal kinetic steps of muscarinic receptor-mediated modulation of phosphoinositides and Kv7.2/7.3 K^+ channels. *J. Gen. Physiol.* 133:347–359. doi:10.1085/jgp.200810075

Jentsch, T.J. 2000. Neuronal KCNQ potassium channels: physiology and role in disease. *Nat. Rev. Neurosci.* 1:21–30. doi:10.1038/35036198

Kharkovets, T., J.P. Hardelin, S. Safieddine, M. Schweizer, A. El-Amraoui, C. Petit, and T.J. Jentsch. 2000. KCNQ4, a K^+ channel mutated in a form of dominant deafness, is expressed in the inner ear and the central auditory pathway. *Proc. Natl. Acad. Sci. USA.* 97:4333–4338. doi:10.1073/pnas.97.8.4333

Koizumi, S., P. Rosa, G.B. Willars, R.A. Challiss, E. Taverna, M. Francolini, M.D. Bootman, P. Lipp, K. Inoue, J. Roder, and A. Jeromin. 2002. Mechanisms underlying the neuronal calcium sensor-1-evoked enhancement of exocytosis in PC12 cells. *J. Biol. Chem.* 277:30315–30324. doi:10.1074/jbc.M201132200

Kubisch, C., B.C. Schroeder, T. Friedrich, B. Lütjohann, A. El-Amraoui, S. Marlin, C. Petit, and T.J. Jentsch. 1999. KCNQ4, a novel potassium channel expressed in sensory outer hair cells, is mutated in dominant deafness. *Cell.* 96:437–446. doi:10.1016/S0092-8674(00)80556-5

Li, Y., N. Gamper, and M.S. Shapiro. 2004. Single-channel analysis of KCNQ K^+ channels reveals the mechanism of augmentation by a cysteine-modifying reagent. *J. Neurosci.* 24:5079–5090. doi:10.1523/JNEUROSCI.0882-04.2004

Li, Y., N. Gamper, D.W. Hilgemann, and M.S. Shapiro. 2005. Regulation of Kv7 (KCNQ) K^+ channel open probability by phosphatidylinositol 4,5-bisphosphate. *J. Neurosci.* 25:9825–9835. doi:10.1523/JNEUROSCI.2597-05.2005

Loew, L.M. 2007. Where does all the PIP_2 come from? *J. Physiol.* 582:945–951. doi:10.1113/jphysiol.2007.132860

Loussouarn, G., I. Baró, and D. Escande. 2006. KCNQ1 K^+ channel-mediated cardiac channelopathies. *Methods Mol. Biol.* 337:167–183.

Mackie, A.R., and K.L. Byron. 2008. Cardiovascular KCNQ (Kv7) potassium channels: physiological regulators and new targets for therapeutic intervention. *Mol. Pharmacol.* 74:1171–1179. doi:10.1124/mol.108.049825

McLaughlin, S., G. Hangyás-Mihályné, I. Zaitseva, and U. Golebiewska. 2005. Reversible - through calmodulin - electrostatic interactions between basic residues on proteins and acidic lipids in the plasma membrane. *Biochem. Soc. Symp.* 72:189–198.

Milosevic, I., J.B. Sørensen, T. Lang, M. Krauss, G. Nagy, V. Haucke, R. Jahn, and E. Neher. 2005. Plasmalemmal phosphatidylinositol-4,5-bisphosphate level regulates the releasable vesicle pool size in chromaffin cells. *J. Neurosci.* 25:2557–2565. doi:10.1523/JNEUROSCI.3761-04.2005

Pan, Z., T. Kao, Z. Horvath, J. Lemos, J.Y. Sul, S.D. Cranstoun, V. Bennett, S.S. Scherer, and E.C. Cooper. 2006. A common ankyrin-G-based mechanism retains KCNQ and NaV channels at electrically active domains of the axon. *J. Neurosci.* 26:2599–2613. doi:10.1523/JNEUROSCI.4314-05.2006

Peroz, D., N. Rodriguez, F. Choveau, I. Baró, J. Mérot, and G. Loussouarn. 2008. Kv7.1 (KCNQ1) properties and channelopathies. *J. Physiol.* 586:1785–1789. doi:10.1113/jphysiol.2007.148254

Rae, J., K. Cooper, P. Gates, and M. Watsky. 1991. Low access resistance perforated patch recordings using amphotericin B. *J. Neurosci. Methods.* 37:15–26. doi:10.1016/0165-0270(91)90017-T

Rajebhosale, M., S. Greenwood, J. Vidugiriene, A. Jeromin, and S. Hilfiker. 2003. Phosphatidylinositol 4-OH kinase is a downstream target of neuronal calcium sensor-1 in enhancing exocytosis in neuroendocrine cells. *J. Biol. Chem.* 278:6075–6084. doi:10.1074/jbc.M204702200

Robbins, J., S.J. Marsh, and D.A. Brown. 2006. Probing the regulation of M (Kv7) potassium channels in intact neurons with membrane-targeted peptides. *J. Neurosci.* 26:7950–7961. doi:10.1523/JNEUROSCI.2138-06.2006

Roche, J.P., R. Westenbroek, A.J. Sorom, B. Hille, K. Mackie, and M.S. Shapiro. 2002. Antibodies and a cysteine-modifying reagent show correspondence of M current in neurons to KCNQ2 and KCNQ3 K^+ channels. *Br. J. Pharmacol.* 137:1173–1186. doi:10.1038/sj.bjp.0704989

Schenzer, A., T. Friedrich, M. Pusch, P. Saftig, T.J. Jentsch, J. Grötzinger, and M. Schwake. 2005. Molecular determinants of KCNQ (Kv7) K^+ channel sensitivity to the anticonvulsant retigabine. *J. Neurosci.* 25:5051–5060. doi:10.1523/JNEUROSCI.0128-05.2005

Selyanko, A.A., J.K. Hadley, I.C. Wood, F.C. Abogadie, T.J. Jentsch, and D.A. Brown. 2000. Inhibition of KCNQ1-4 potassium channels expressed in mammalian cells via M_1 muscarinic acetylcholine receptors. *J. Physiol.* 522:349–355. doi:10.1111/j.1469-7793.2000.t01-2-00349.x

Shapiro, M.S., J.P. Roche, E.J. Kaftan, H. Cruzblanca, K. Mackie, and B. Hille. 2000. Reconstitution of muscarinic modulation of the KCNQ2/KCNQ3 $K(^+)$ channels that underlie the neuronal M current. *J. Neurosci.* 20:1710–1721.

Suh, B.C., and B. Hille. 2002. Recovery from muscarinic modulation of M current channels requires phosphatidylinositol 4,5-bisphosphate synthesis. *Neuron.* 35:507–520. doi:10.1016/S0896-6273(02)00790-0

Suh, B.C., L.F. Horowitz, W. Hirdes, K. Mackie, and B. Hille. 2004. Regulation of KCNQ2/KCNQ3 current by G protein cycling: the kinetics of receptor-mediated signaling by Gq. *J. Gen. Physiol.* 123:663–683. doi:10.1085/jgp.200409029

Suh, B.C., T. Inoue, T. Meyer, and B. Hille. 2006. Rapid chemically induced changes of PtdIns(4,5)P2 gate KCNQ ion channels. *Science.* 314:1454–1457. doi:10.1126/science.1131163

Wang, H.S., Z. Pan, W. Shi, B.S. Brown, R.S. Wymore, I.S. Cohen, J.E. Dixon, and D. McKinnon. 1998. KCNQ2 and KCNQ3 potassium channel subunits: molecular correlates of the M-channel. *Science.* 282:1890–1893. doi:10.1126/science.282.5395.1890

Winks, J.S., S. Hughes, A.K. Filippov, L. Tatulian, F.C. Abogadie, D.A. Brown, and S.J. Marsh. 2005. Relationship between membrane phosphatidylinositol-4,5-bisphosphate and receptor-mediated inhibition of native neuronal M channels. *J. Neurosci.* 25:3400–3413. doi:10.1523/JNEUROSCI.3231-04.2005

Xu, C., J. Watras, and L.M. Loew. 2003. Kinetic analysis of receptor-activated phosphoinositide turnover. *J. Cell Biol.* 161:779–791. doi:10.1083/jcb.200301070

Zaika, O., G.P. Tolstykh, D.B. Jaffe, and M.S. Shapiro. 2007. Inositol triphosphate-mediated Ca^{2+} signals direct purinergic P2Y receptor regulation of neuronal ion channels. *J. Neurosci.* 27:8914–8926. doi:10.1523/JNEUROSCI.1739-07.2007

Zaika, O., C.C. Hernandez, M. Bal, G.P. Tolstykh, and M.S. Shapiro. 2008. Determinants within the turret and pore-loop domains of KCNQ3 K^+ channels governing functional activity. *Biophys. J.* 95:5121–5137. doi:10.1529/biophysj.108.137604

Zhang, H., L.C. Craciun, T. Mirshahi, T. Rohács, C.M. Lopes, T. Jin, and D.E. Logothetis. 2003. $PIP(_2)$ activates KCNQ channels, and its hydrolysis underlies receptor-mediated inhibition of M currents. *Neuron.* 37:963–975. doi:10.1016/S0896-6273(03)00125-9

Zhao, X., P. Várnai, G. Tuymetova, A. Balla, Z.E. Tóth, C. Oker-Blom, J. Roder, A. Jeromin, and T. Balla. 2001. Interaction of neuronal calcium sensor-1 (NCS-1) with phosphatidylinositol 4-kinase beta stimulates lipid kinase activity and affects membrane trafficking in COS-7 cells. *J. Biol. Chem.* 276:40183–40189.

Zheng, Q., J.A. Bobich, J. Vidugiriene, S.C. McFadden, F. Thomas, J. Roder, and A. Jeromin. 2005. Neuronal calcium sensor-1 facilitates neuronal exocytosis through phosphatidylinositol 4-kinase. *J. Neurochem.* 92:442–451. doi:10.1111/j.1471-4159.2004.02897.x